

Title: ^{18}F -5-fluoro-aminosuberic acid (FASu) as a potential tracer to gauge oxidative stress in breast cancer models

Running Title: ^{18}F -FASu for Oxidative Stress Imaging

Hua Yang¹, Silvia Jenni², Milena Colovic^{1, 3}, Helen Merkens², Carlee Poleschuk¹, Isabel Rodrigo¹, Qing Miao¹, Bruce F. Johnson⁴, Michael J. Rishel⁴, Vesna Sossi⁵, Jack M. Webster⁴, François Bénard^{2, 3}, Paul Schaffer^{1, 3, 6}

Authors' Affiliations: ¹Life Sciences, TRIUMF, Vancouver, Canada; ²The British Columbia Cancer Agency, Vancouver, Canada; ³Department of Radiology, University of British Columbia, Vancouver, Canada; ⁴GE Global Research, Niskayuna, NY, USA; ⁵Department of Physics & Astronomy, University of British Columbia, Vancouver, Canada; and ⁶Department of Chemistry, Simon Fraser University, Vancouver, Canada

For correspondence or reprints contact: Paul Schaffer, Life Sciences, TRIUMF, 4004 Wesbrook Mall, Vancouver, Canada, V6T 2A3. Phone: +1-604-222-7696; Fax: +1-604-222-1074; E-mail: pschaffer@triumf.ca

First Author: Hua Yang, Life Sciences, TRIUMF, 4004 Wesbrook Mall, Vancouver, Canada, V6T 2A3. Phone: +1-604-222-1047 ext. 6756; Fax: +1-604-222-1074; E-mail: hyang@triumf.ca

Key words: Oxidative Stress, System x_c^- , PET, tumor imaging, F-18

Word counts: Abstract: 303; article: 4937

Disclosure

B. F. Johnson and M. J. Rishel are employed by GE Global Research.

ABSTRACT

The cystine transporter (system x_c^-) is an antiporter of cystine and glutamate. It has relatively low basal expression in most tissues and becomes upregulated in cells under oxidative stress (OS) as one of the genes expressed in response to the antioxidant response element (ARE) promoter. We have developed ^{18}F -5-fluoro-aminosuberic acid (FASu), a Positron Emission Tomography (PET) tracer that targets system x_c^- . The goal of this study was to evaluate ^{18}F -FASu as a specific gauge for system x_c^- activity *in vivo* and its potential for breast cancer imaging. **Methods:** ^{18}F -FASu specificity towards system x_c^- was studied by cell inhibition assay, cellular uptake following OS induction with diethyl maleate (DEM), with and without anti-xCT siRNA knockdown, *in vitro* uptake studies and *in vivo* uptake in a system x_c^- transduced xenograft model. In addition, radiotracer uptake was evaluated in three separate breast cancer models MDA-MB-231, MCF-7 and ZR-75-1. **Results:** Reactive oxygen species (ROS)-inducing DEM increased glutathione levels and ^{18}F -FASu uptake, while gene knockdown with anti-xCT siRNA led to decreased tracer uptake. ^{18}F -FASu uptake was robustly inhibited by system x_c^- inhibitors or substrates, while the uptake was significantly higher in transduced cells and tumors expressing xCT compared to the wild type HEK293T cells and tumors ($p < 0.0001$ for cells, $p = 0.0086$ for tumors). ^{18}F -FASu demonstrated tumor uptake in all three breast cancer cell lines studied. Among them, triple negative breast cancer MDA-MB-231 had the highest tracer uptake ($p = 0.0058$ when compared with MCF-7; $p < 0.0001$ when compared with ZR-75-1), which also has the highest xCT mRNA level. **Conclusions:** ^{18}F -FASu as a system x_c^- substrate is a specific PET tracer for functional monitoring of system x_c^- and OS imaging. By enabling non-invasive analysis of x_c^- responses *in vivo*, this biomarker

may serve as a valuable target for the diagnosis and treatment monitoring of certain breast cancers.

INTRODUCTION

OS is the result of an imbalance in cellular ROS and antioxidants and the cellular response to OS has been recognized as a critical regulatory mechanism for cancer and cancer stem cells (1,2). During OS, the expression of ARE-regulated genes, including the key subunit of the x_c^- transporter system (xCT, *SLC7A11*), are upregulated through the KEAP1, Nrf2 pathway (3), which leads to the increased biosynthesis of glutathione. Glutathione is the predominant endogenous cellular antioxidant and plays a critical role in the defensive cellular response to OS by neutralizing free radicals and reactive oxygen and nitrogen compounds (4,5). The rate limiting precursor for glutathione synthesis is cysteine, which cells can obtain through uptake of its oxidized form cystine. System x_c^- plays its primary role by importing cystine to provide cysteine for glutathione synthesis in response to OS. In addition, x_c^- serves as a mediator of physiological redox potential across the cell membrane, working in concert with other transporters to establish an appropriate level of cystine/cysteine on both sides of the cell membrane (4). System x_c^- transporter activity and expression in normal cells is typically low, but is significantly upregulated in cells under OS (6). Thus, x_c^- transporter activity is a promising platform from which to develop targeted treatments for cancer, with several groups exploring the feasibility of targeting the unique x_c^- subunit, xCT, for cancer therapeutics (7-12). Tumors with increased xCT activity are associated with resistance to chemotherapy, and inhibition of xCT has been shown to sensitize cancer cells to chemotherapeutic drugs such as

doxorubicin (12,13), gemcitabine, celestrol (14) and etoposide (15). In addition, immunohistochemical analysis of xCT protein expression has been shown to correlate with tumor staging (16). Consequently, the x_c^- transporter may be a useful diagnostic target for cancer imaging and utilizing this transporter as a functional reporter of OS may provide valuable information for clinical cancer management, including early detection, staging, patient stratification, monitoring of response to therapy and the development of new therapeutics.

We developed a cystine/glutamate analog, ^{18}F - 5-fluoro-aminosuberic acid (FASu), as a potent cystine transporter substrate with the goal of assessing its potential as a diagnostic tracer of OS via x_c^- activity (17). We previously reported the design, synthesis and *in vivo* evaluation of ^{18}F -FASu in EL4 and SKOV3 tumor models (17). Our previous study on ^{18}F -FASu demonstrated high tumor to background ratios in both tumor types, prompting us to evaluate the specificity of this tracer for xCT and its potential utility in the detection and monitoring of other tumor types. Herein we report the *in vitro* and *in vivo* studies that establish ^{18}F -FASu uptake via system x_c^- in three breast cancer models. Our studies include MCF-7, ZR-75-1 and a triple negative breast cancer (TNBC) model MDA-MB-231, representing a range of breast cancer subtypes. We are particularly interested in TNBC, which maintains low expression levels of estrogen, progesterone and HER2 receptors and is typically associated with poor patient outcomes, including lower overall survival rates as well as aggressive and early recurrence (18). The cystine transporter is commonly expressed and functional in TNBC, and inhibition with sulfasalazine can increase ROS and slow cell growth in MDA-MB-231 tumors (8). An exploratory clinical study with ^{18}F -FSPG ((4S)-4-(3- ^{18}F -fluoropropyl)-L-glutamate), a glutamate analog that targeted system x_c^- , showed significant uptake in a subset of breast cancer lesions (19). The purpose of this study

was to evaluate the relationship between system x_c^- and ^{18}F -FASu uptake in models of human breast cancer.

MATERIALS AND METHODS

Chemistry and radiochemistry

The radiolabeling precursor di-*tert*-butyl 2-((bis-*tert*-butoxycarbonyl)amino)-5-(tosyloxy)octanedioate (compound **1**, Fig. 1) was synthesized on a GE TRACERLab FXFN module using our reported method (17). Radiofluorination was carried out by nucleophilic substitution followed by acidic deprotection. See Supplemental Data for details pertaining to the radiosynthesis and *in vitro* and *in vivo* stability studies.

Cell culture and uptake experiments

The HEK-293T cell line was purchased from Clontech Laboratories. The ZR-75-1 cell line was purchased from ATCC[®]. The MCF-7 cell line was obtained as a gift from Dr. C. Kent Osborne (Baylor College of Medicine, Houston, TX) and authenticated by DDC Medical. The MDA-MD-231 cell line was obtained as a gift from Dr. Connie Eaves (Vancouver, BC), and authenticated by DDC Medical.

The MDA-MB-231 cell line was cultured in complete DMEM (with 4500 mg/L glucose + 10% FBS + 1% Penicillin/Streptomycin). ZR-75-1 was cultured in complete RPMI-1640 (with 10% FBS + 1% Penicillin/Streptomycin). MCF-7 was cultured in complete DMEM with 1% Minimum Essential Medium non-essential amino acid solution. Cells were maintained in 10 cm tissue culture dishes in a humidified incubator at 37°C with 5% CO₂ and routinely sub cultured at ~95% confluency.

For uptake studies, cells were seeded into 24 well plates (1×10^5 cells/mL) such that confluency was achieved the next day. Each plate was washed three times with cold Hepes-HBSS and then 0.148 MBq ^{18}F -FASu in 400 μL Hepes-HBSS was added. Cell numbers were established from a single well using a Moxi™ Z Mini Automated Cell Counter. Subsequently the samples were incubated at 37°C with orbital shaking for the indicated duration. After incubation, supernatants were removed and cells were washed two times with cold Hepes-HBSS. 400 μL of 1 M NaOH were added to the cells and the NaOH lysate was collected 10 min later. 25 μL of the lysate was used to assess the protein concentration using a Pierce™ BCA Protein Assay Kit (Thermo Fisher Scientific). The activity in the solution and lysate was measured using a PerkinElmer Wizard 2480 gamma counter and normalized to the protein concentration.

For DEM-induced OS experiments, DEM was added at various concentrations approximately 24 hours before harvesting. The uptake study was conducted using the method described above.

For amino acid transporter inhibition experiments, all chemicals were purchased from Sigma-Aldrich and used without further modification. L-Glu, D-Asp, 2-Amino-2-norbornanecarboxylic acid (BCH), L-Leu and L-Ser were used at 2 mM and SSZ at 1.0 mM concentration. The inhibitors were added to MDA-MB-231 cells and incubated with ^{18}F -FASu at 37°C with 5% CO_2 for 60 min.

siRNA knockdown experiments

MDA-MB-231 cells were seeded at 1×10^5 cells/mL in a 24-well plate with complete DMEM 24 hours prior to transfection with siRNA (xCT siRNA and non-targeting control siRNA both from Santa Cruz Biotechnologies). Cells were transfected at 80%

confluency with a mixture containing 25 nM siRNA, 1.5 μ L TransitIT siQuest transfection reagent (Mirus), and Opti-MEM reduced serum medium prepared and added according to the manufacturers' directions. The cells were left to incubate at 37°C with 5% CO₂ for 24 hours. Then, 0.1 mM DEM was added to the cells and incubated an additional 24 hours, followed by a tracer uptake study using the method described above.

Glutathione quantification

Glutathione content was determined, in triplicate, using the Thiol Detection Assay Kit from Cayman Chemical per manufacturer's instructions. The fluorescent signal was recorded using a FlexStation® 3 spectrophotometer (Molecular Devices). The glutathione content in each sample was estimated from the standard curve and normalized to protein content.

HEK::xCT cell line

The lentiviral plasmid Lv205 (pReceiver-ORF-IRES-eGFP-IRES-Puro) containing the ORF of human *SLC7A11* (GeneCopoeia) was used to generate virus particles using a second-generation packaging system. HEK-293T cells grown in antibiotic free media were transduced using 3:1 plasmids (Lv205-xCT and the packaging plasmids) to transduction reagent ratio following the manufacturer's instructions (transit-LT1, Mirus) and incubated at 37°C. The cell culture supernatant containing the virus was harvested 48 and 72 h after the transduction, passed through a 0.45 μ m low protein binding filter and directly incubated on HEK-293T cells grown to 50% confluency. After 48 h of incubation, cells were passaged three times with complete medium before selecting the cells harboring the xCT-plasmid with puromycin added at 3 μ g/mL.

Quantitative-PCR (qPCR)

Transcriptional expression of xCT (*SLC7A11*) in MDA-MB-231, MCF-7 and ZR-75 cells was determined relative to hypoxanthine phosphoribosyltransferase 1 (*HPRT1*). Total RNA was purified using the GenElute Mammalian Total RNA Miniprep Kit (Sigma), treated with amplification grade DNase I (Sigma), and measured using a NanoDrop™ spectrophotometer. 50 ng of total RNA from each sample was reverse transcribed in a 20 µL reaction using SuperScript® VILO™ cDNA synthesis kit (Invitrogen). qPCR was set up in 384-well plates and performed on a QuantStudio 6K Flex Real-Time PCR system. Each 10 µL reaction contains 1 µL template cDNA, 500 µM forward and reverse primers and 250 µM probe (IDT), and 1x SsoAdvanced™ Universal Probes Supermix (Bio Rad). MDA-MB-231 was assayed in triplicate; MCF-7 and ZR-75 were assayed in 2x triplicates. The concentration of each target was determined by interpolating the Ct value from respective standard curves of known concentrations.

The information of primer and probes, the construction of *SLC7A11* and *HPRT1* standard curves, and cycling conditions for both PCR and qPCR can be found in Supplemental Data.

Small-animal PET and biodistribution studies

All animal experiments were conducted in accordance with the guidelines established by the Canadian Council on Animal Care and approved by the Animal Care Committee of the University of British Columbia. Female immunodeficient RAG2M mice (12 weeks to 14 weeks, 19 g to 26 g) were obtained from an in-house breeding colony at the Animal Resource Centre of the British Columbia Cancer Research Centre.

MDA-MB-231, ZR-75-1, MCF-7 and HEK-293T tumors were inoculated subcutaneously with $5-10 \times 10^6$ cells in matrigel on the dorsal flank of the mice. MCF-7 and ZR-75-1 required implantation of a 17β -estradiol releasing pellet (0.36 mg / 60 days, Innovative Research of America) 7 days before inoculation.

Once palpable tumors measuring ~ 7-10 mm were obtained (~2-4 weeks), mice were anesthetized by 2% isoflurane inhalation and intravenously injected with ~3.7 MBq of ^{18}F -FASu. The activity in the syringe was counted before and after injection to determine the exact injected dose.

For blocking experiments, the radiotracer was co-injected with 100 mg/kg of nonradioactive aminosuberic acid (ASu). After injections, mice were allowed to recover and roam freely in cages for 60 min. Animals were then anesthetized by 2% isoflurane inhalation and then euthanized by CO_2 at various time points. Blood was promptly withdrawn via a cardiac puncture, and the tissues of interest were harvested, rinsed in PBS, blotted dry and weighed. The radioactivity of the collected mouse tissues was counted on a gamma counter and expressed as the percentage injected dose per gram of tissue (%ID/g).

Mice destined for a static emission scan were anesthetized with 2% isoflurane inhalation 1 or 2 h after intravenous injection of the tracer and placed on the scanner. A baseline computed tomography (CT) scan was obtained for localization and attenuation correction. During acquisition, anesthesia was maintained and the mice were kept warm with a heating pad. A single static emission scan was acquired for 15 min. Afterwards, the mice were euthanized and the organs harvested for biodistribution as described above.

Statistical Analysis

Test statistics and p-values were calculated using Minitab Express analysis software. The descriptive statistics are reported as mean \pm standard deviation when applicable. Comparison of means was conducted using a two-sample t-test, assuming equal variance. A p value of <0.05 was considered significant.

RESULTS

***In vitro* uptake specificity studies**

In order to examine the uptake specificity of ^{18}F -FASu in cancer cell lines, we studied tracer uptake in the TNBC cell line MDA-MB-231 at 60 min in the presence of substrates or inhibitors of common amino acids (Table 1). The results showed no statistically significant difference between the uptake with or without D-Asp, L-Leu and BCH, while uptake increased to $126\pm 14\%$ in the presence of L-Ser, indicating the uptake is not through EAAT, system L, B⁰, B⁰⁺, A or ACS. Tracer uptake was suppressed only by L-Glu, L-ASu and SSZ, all of which are substrates or inhibitors of system x_c⁻, indicating that amongst the transporters analyzed here, uptake of ^{18}F -FASu is specific to system x_c⁻.

It has been reported that DEM, as an electrophilic oxidant, induces xCT expression and concomitantly increases cellular glutathione levels (20-22). Cellular uptake of ^{18}F -FASu showed a dose dependent increase after DEM incubation (Fig. 2A). The uptake gradually increased with the addition of 2, 5, 10, and 20 μM DEM and reached a plateau at higher concentration. Cellular glutathione levels showed a similar trend over

the same DEM concentration range (Fig. 2B). These results indicate that with increased OS inducer, higher levels of glutathione are maintained, which correlates with higher tracer uptake. In contrast, when system x_c^- was knocked down upon incubation with xCT siRNA, ^{18}F -FASu uptake decreased significantly compared to the cells incubated with non-targeting control siRNA ($62\pm 5\%$, $p=0.0017$) or without siRNA ($68\pm 3\%$, $p=0.0010$, Fig. 2C).

Among the two sub-units of system x_c^- , xCT is unique to system x_c^- , leading us to establish a positive control cell line by transducing HEK293T (HEK WT) cells with an xCT expression vector (HEK::xCT). The cell uptake of ^{18}F -FASu at 1 h in HEK::xCT cells was $5.4\pm 0.5 \times 10^4$ cpm/ 10^5 cells, while the uptake in WT cells was only $6.5\pm 1.1 \times 10^3$ cpm/ 10^5 cells ($p<0.0001$, Fig. 2D) under the same conditions.

***In vivo* uptake specificity study in xCT transduced tumor xenograft**

A biodistribution study was also performed using female mice inoculated with both HEK::xCT and HEK WT tumors. The average tumor uptake was 10.4 ± 4.1 %ID/g ($n=5$) for HEK::xCT and 4.0 ± 0.6 %ID/g ($n=5$) for HEK WT (Fig. 3). Both tumors exhibited lower uptake when co-injected with aminosuberic acid (ASu) as a blocking agent (Fig. 3A). HEK::xCT uptake decreased by 67% ($n=3$), while the HEK WT tumor saw a 54% decline ($n=3$). Fig. 3B shows a static PET image acquired at 1 hour post injection, which confirmed higher uptake in HEK::xCT and lower uptake in HEK WT. In addition to tumor, kidneys (11.2 ± 4.9 %ID/g) and bladder, appreciable uptake was also observed in the pancreas (18.0 ± 2.8 %ID/g), spleen (3.4 ± 1.3 %ID/g), ovaries (4.3 ± 2.6 %ID/g) and uterus (4.1 ± 3.9 %ID/g); all of which decreased with co-injection of ASu. The uptake in blood (0.43 ± 0.11 %ID/g) and muscles (0.17 ± 0.02 %ID/g) were much lower in comparison to tumors.

Human breast cancer cell lines *in vitro* data

MDA-MB-231, MCF-7 and ZR-75-1 have modest to low reported xCT mRNA expression among the breast cancer cell lines (23). We measured the copy number of *SLC7A11* (xCT) transcripts in MDA-MB-231, MCF-7 and ZR-75-1 cell lines using absolute qPCR (Fig. 4B). MDA-MB-231 cells expressed the highest *SLC7A11* level (842±45 copies/μL) compared to the other two cell lines (237±80 copies/μL for MCF-7, 314±54 copies/μL for ZR-75-1). Uptake of ¹⁸F-FASu in the cells is shown to increase over 60 min (Fig. 4A). MDA-MB-231 had the highest uptake compared to the other two cell lines, whereas MCF-7 had the lowest uptake over 60 min. This is consistent with the trend of the mRNA expression level measured. For MDA-MB-231 and MCF-7, the uptake was suppressed by 86±13% and 82±9% (n=4) respectively by adding the system x_c⁻ inhibitor sulfasalazine (SSZ), whereas the uptake in ZR-75-1 was only suppressed by 58±5% (n=4) with SSZ, which indicates that ZR-75-1 cells may exhibit an additional alternative, unknown, uptake mechanism.

Human breast cancer tumor xenograft *in vivo* data

The *in vivo* MDA-MB-231 tumor uptake in RAG2M mice at 5, 30, 60 and 120 min post injection were studied. The tumor-to-blood ratio continuously increased to 7.2 at 120 min (Fig. 5A). The tumor-to-muscle ratio increased to 8.1 at 60 min, and remained at this level through to 120 min post injection. PET imaging results at 2 h post injection along with the biodistribution analysis of ¹⁸F-FASu in MDA-MB-231 tumor bearing mice are shown in Fig. 5B and 5C. The highest organ uptake was in the pancreas, likely due to the high xCT level in this organ (24). Kidneys also had high uptake, suggesting a preference of renal clearance for this radiotracer. Other organs exhibiting high

uptake included the spleen, uterus and ovaries, which are also reported to have relatively higher levels of xCT expression (25).

At 2 hour post injection, the tumor uptake values in MDA-MB-231, MCF-7 and ZR-75-1 were 1.38 ± 0.27 %ID/g (n=9), 1.01 ± 0.20 %ID/g (n=8) and 0.75 ± 0.14 %ID/g (n=8) respectively (Fig. 5D, whole body biodistribution see Supplemental Data). The tumor uptake in MDA-MB-231 was higher than in ZR-75-1 and MCF-7 ($p < 0.0001$ when compared to ZR-75-1, $p = 0.0058$ when compared to MCF-7), consistent with MDA-MB-231's higher mRNA expression level measured in cells.

DISCUSSION

Clinical functional imaging in oncology has long relied on the analysis of enhanced glucose utilization, as monitored by ^{18}F -FDG, for tumor detection. The success of ^{18}F -FDG is due, in part, to the fact that it is a substrate for a ubiquitous cellular pathway and holds relevance for a wide number of clinical indications. OS is a common pathogenic process present in many diseases and the cystine transporter, as part of the antioxidant response element, provides a biomarker for OS imaging. A specific radiotracer driven by OS may have value in detection, staging and therapy response monitoring (4). Herein we report the use of ^{18}F -FASu as a cystine/glutamate analog for monitoring system x_c⁻ in three models of breast cancer. The goal was to evaluate ^{18}F -FASu as an indirect, non-invasive indicator of cellular OS via system x_c⁻.

Using a transduced HEK::xCT cell line we established a positive control to help examine the specificity of ^{18}F -FASu towards system x_c⁻. HEK::xCT showed much higher ^{18}F -FASu cellular uptake compared to HEK WT ($p < 0.0001$). Studies in mice

bearing both HEK::xCT and HEK WT tumors demonstrated significantly higher uptake in HEK::xCT tumor than in HEK WT tumor ($p=0.0086$).

We also studied tracer specificity using cell based uptake experiments and inhibition assays in a TNBC cell line MDA-MB-231. We observed strong inhibition with L-Cys and L-Glu, two natural substrates of system x_c^- , and significant blocking in the presence of SSZ, a known x_c^- inhibitor. There was no inhibition with D-Asp, L-Leu, L-Ser and BCH, establishing a negligible substrate role for systems L, A, ACS, B^0 , B^{0+} and EAAT transport activity.

Additional evidence for specificity came from xCT siRNA knockdown studies that show reduced tracer uptake when cells were treated with anti-xCT siRNA but not with control siRNA. Finally, in conditions where OS was induced by DEM, we have shown that both intracellular glutathione levels and tracer uptake increases with increased DEM dose. The results indicate a positive correlation between cellular OS and ^{18}F -FASu uptake.

We then applied this tracer to assess system x_c^- in three different breast cancer cell lines: ZR-75-1 (ER+/PR+/Her2-), MCF-7 (ER+/PR+/Her2-) and MDA-MB-231 (ER-/PR-/Her2-). We found the TNBC cell line MDA-MB-231 had higher tracer uptake *in vitro* and higher tumor uptake *in vivo*. These results further confirm that ^{18}F -FASu can be used as a non-invasive indicator of system x_c^- activity and also validate system x_c^- as a biomarker across different breast cancers sub-types. Although ^{18}F -FDG PET has shown its potential to diagnose breast cancers, variable sensitivity and specificity, along with inconsistencies for small and low-grade lesions limits its clinical use to detect these tumors (26). As FDG is not used for primary breast cancer detection, alternative biomarkers could provide a different perspective to meet the challenges of

diagnosing and monitoring breast cancer sub-types. Previous studies have established TNBC as having higher xCT expression and higher cystine consumption, which supports the potential utility of this biomarker for xCT-PET in clinical breast cancer management (8).

¹⁸F-FSPG is another system xc⁻ PET tracer which has been used in patients with non-small cell lung, breast, and liver cancers (19,27). While similar in target, these two tracers maintain key differences in their respective structural arrangement of the carbon backbone. FSPG maintains a 4-bond separation between carboxyl groups, while FASu has seven, making the latter closer in structural orientation to cystine. We presume the affinity and specificity of the two tracers towards system xc⁻ will be different and work is currently underway to compare these tracers in order to establish their respective value as specific xCT transporter imaging agents.

CONCLUSION

In conclusion, the data within support our hypothesis for using ¹⁸F-FASu as a tracer to monitor system xc⁻ *in vivo*. ¹⁸F-FASu is a specific tracer for system xc⁻ in three separate human breast cancer models. Further studies are underway to better understand the effect of optical purity on tumor uptake and image quality. Experiments are also underway to compare ¹⁸F-FASu to ¹⁸F-FDG (OS vs glucose metabolism) and ¹⁸F-FSPG (structurally unique xc⁻ tracers). We expect that the ability to assess xc⁻ via PET will contribute to an understanding of its role in disease and speed development of interventions that moderate OS-related disease processes.

ACKNOWLEDGMENTS

We thank TRIUMF TR13 cyclotron operators, BC Cancer Research Centre PET imaging staff, Lily Southcott, Iulia Dude and Sofya Langman for their technical help. We thank the financial support from CIHR (201403COP, 329895). MJR, BFJ and JMW were supported by NIH 5R01EB014250-04. TRIUMF receives federal funding via a contribution agreement with the National Research Council of Canada.

REFERENCES

1. Nagano O, Okazaki S, Saya H. Redox regulation in stem-like cancer cells by CD44 variant isoforms. *Oncogene*. 2013;32:5191-5198.
2. Dayem AA, Choi HY, Kim JH, Cho SG. Role of oxidative stress in stem, cancer, and cancer stem cells. *Cancers (Basel)*. 2010;2:859-884.
3. Nguyen T, Nioi P, Pickett CB. The Nrf2-antioxidant response element signaling pathway and its activation by oxidative stress. *J Biol Chem*. 2009;284:13291-13295.
4. Conrad M, Sato H. The oxidative stress-inducible cystine/glutamate antiporter, system x(c)(-): cystine supplier and beyond. *Amino Acids*. 2012;42:231-246.
5. Bridges RJ, Natale NR, Patel SA. System xc- cystine/glutamate antiporter: an update on molecular pharmacology and roles within the CNS. *Brit J Pharmacol*. 2012;165:20-34.
6. Ishii T, Sato H, Miura K, Sagara J, Bannai S. Induction of cystine transport activity by stress. *Ann N Y Acad Sci*. 1992;663:497-498.
7. Lo M, Wang YZ, Gout PW. The x(c)(-) cystine/glutamate antiporter: A potential target for therapy of cancer and other diseases. *J Cell Physiol*. 2008;215:593-602.
8. Timmerman LA, Holton T, Yuneva M, et al. Glutamine sensitivity analysis identifies the xCT antiporter as a common triple-negative breast tumor therapeutic target. *Cancer Cell*. 2013;24:450-465.
9. Yoshikawa M, Tsuchihashi K, Ishimoto T, et al. xCT inhibition depletes CD44v-expressing tumor cells that are resistant to EGFR-targeted therapy in head and neck squamous cell carcinoma. *Cancer Res*. 2013;73:1855-1866.

- 10.** Dai L, Cao YY, Chen YH, Parsons C, Qin ZQ. Targeting xCT, a cystine-glutamate transporter induces apoptosis and tumor regression for KSHV/HIV-associated lymphoma. *J Hematol Oncol.* 2014;7:30.

- 11.** Doxsee DW, Gout PW, Kurita T, et al. Sulfasalazine-induced cystine starvation: Potential use for prostate cancer therapy. *Prostate.* 2007;67:162-171.

- 12.** Lay JD, Hong CC, Huang JS, et al. Sulfasalazine suppresses drug resistance and invasiveness of lung adenocarcinoma cells expressing AXL. *Cancer Res.* 2007;67:3878-3887.

- 13.** Narang VS, Pauletti GM, Gout PW, Buckley DJ, Buckley AR. Sulfasalazine-induced reduction of glutathione levels in breast cancer cells: Enhancement of growth-inhibitory activity of doxorubicin. *Chemotherapy.* 2007;53:210-217.

- 14.** Pham AN, Blower PE, Alvarado O, Ravula R, Gout PW, Huang Y. Pharmacogenomic approach reveals a role for the x(c)(-) cystine/glutamate antiporter in growth and celastrol resistance of glioma cell lines. *J Pharmacol Exp Ther.* 2010;332:949-958.

- 15.** Muerkoster S, Arlt A, Witt M, et al. Usage of the NF-kappa B inhibitor sulfasalazine as sensitizing agent in combined chemotherapy of pancreatic cancer. *Int J Cancer.* 2003;104:469-476.

- 16.** Qin ZQ, Freitas E, Sullivan R, et al. Upregulation of xCT by KSHV-Encoded microRNAs Facilitates KSHV Dissemination and Persistence in an Environment of Oxidative Stress. *Plos Pathog.* 2010;6.

- 17.** Webster JM, Morton CA, Johnson BF, et al. Functional Imaging of Oxidative Stress with a Novel PET Imaging Agent, F-18-5-Fluoro-L- Aminosuberic Acid. *J Nucl Med.* 2014;55:657-664.

- 18.** Karihtala P, Kauppila S, Soini Y, Arja-Jukkola-Vuorinen. Oxidative stress and counteracting mechanisms in hormone receptor positive, triple-negative and basal-like breast carcinomas. *Bmc Cancer.* 2011;11.

- 19.** Baek S, Choi CM, Ahn SH, et al. Exploratory clinical trial of (4S)-4-(3-[18F]fluoropropyl)-L-glutamate for imaging xC- transporter using positron emission tomography in patients with non-small cell lung or breast cancer. *Clin Cancer Res.* 2012;18:5427-5437.
- 20.** Bannai S. Induction of Cystine and Glutamate Transport Activity in Human-Fibroblasts by Diethyl Maleate and Other Electrophilic Agents. *J Biol Chem.* 1984;259:2435-2440.
- 21.** Hosoya KI, Tomi M, Ohtsuki S, et al. Enhancement of L-cystine transport activity and its relation to xCT gene induction at the blood-brain barrier by diethyl maleate treatment. *J Pharmacol Exp Ther.* 2002;302:225-231.
- 22.** Sasaki H, Sato H, Kuriyama-Matsumura K, et al. Electrophile response element-mediated induction of the cystine/glutamate exchange transporter gene expression. *J Biol Chem.* 2002;277:44765-44771.
- 23.** Barretina J, Caponigro G, Stransky N, et al. The Cancer Cell Line Encyclopedia enables predictive modelling of anticancer drug sensitivity. *Nature.* 2012;483:603-607.
- 24.** Lo M, Ling V, Wang YZ, Gout PW. The x(c)(-) cystine/glutamate antiporter: a mediator of pancreatic cancer growth with a role in drug resistance. *Br J Cancer.* 2008;99:464-472.
- 25.** Kapushesky M, Emam I, Holloway E, et al. Gene Expression Atlas at the European Bioinformatics Institute. *Nucleic Acids Res.* 2010;38:D690-D698.
- 26.** Rosen EL, Eubank WB, Mankoff DA. FDG PET, PET/CT, and breast cancer imaging. *Radiographics.* 2007;27:S215-S229.
- 27.** Koglin N, Mueller A, Berndt M, et al. Specific PET imaging of xC- transporter activity using a (1)(8)F-labeled glutamate derivative reveals a dominant pathway in tumor metabolism. *Clin Cancer Res.* 2011;17:6000-6011.

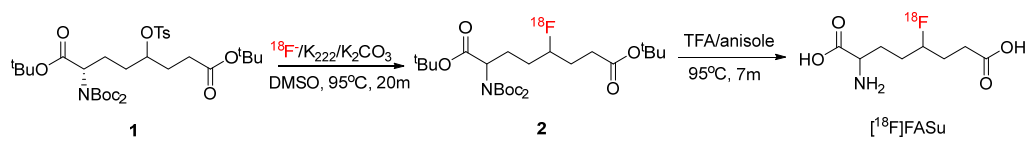


FIGURE 1. Radiosynthesis of ^{18}F -FASu.

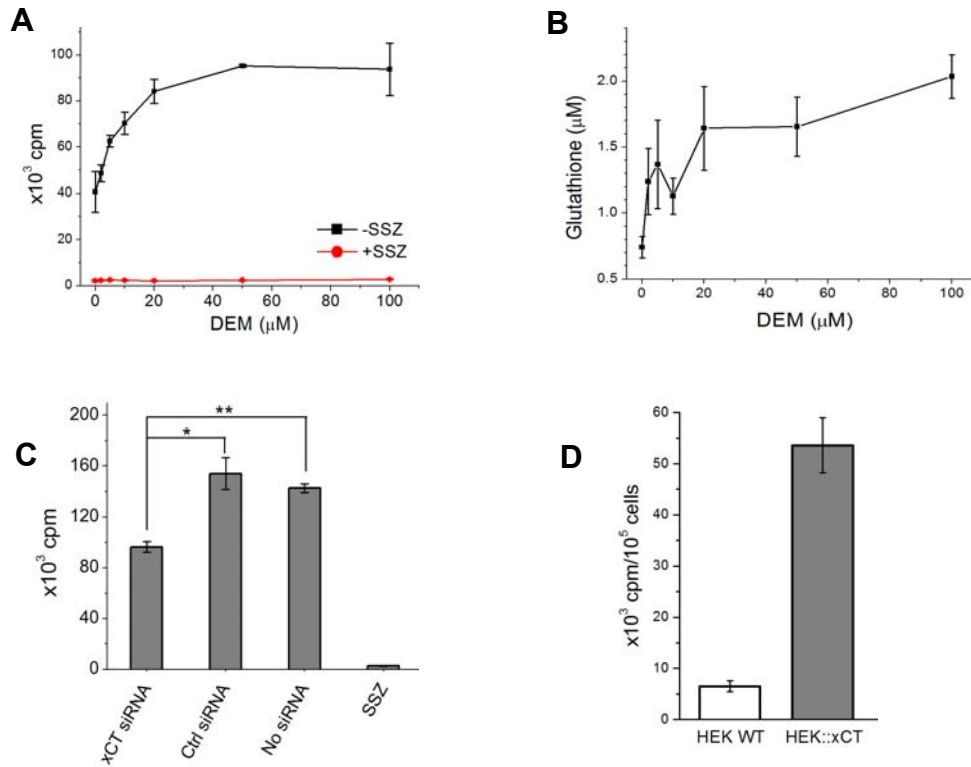
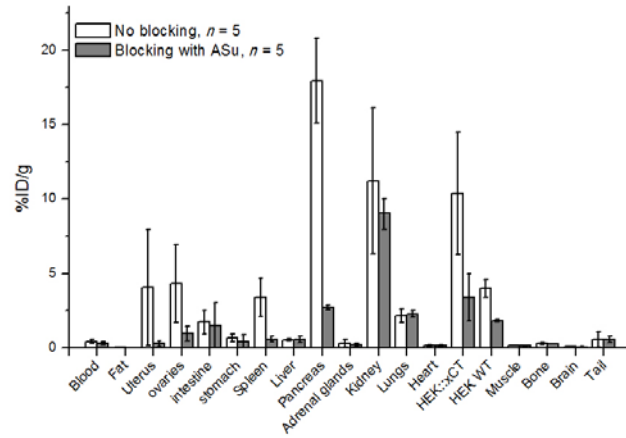


FIGURE 2. ¹⁸F-FASu uptake specificity study. A, ¹⁸F-FASu uptake in MDA-MB-231 cells at 60 min with addition of DEM at 0, 2, 5, 10, 20, 50, 100 μM to induce the OS; B, glutathione concentration in MDA-MB-231 cells with addition of DEM at 0, 2, 5, 10, 20, 50, 100 μM; C, uptake in MDA-MB-231 cells after addition of xCT siRNA, control siRNA, no siRNA or 500 μM SSZ, *p=0.0017, **p=0.0010; D, uptake in HEK WT and HEK::xCT cells at 60 min, p<0.0001.

A



B

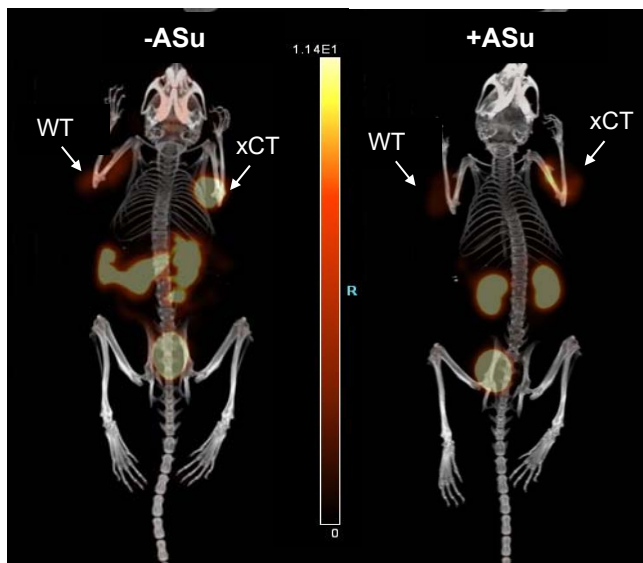


FIGURE 3. A, biodistribution with (n=5) and without (n=5) co-injection of 100 mg/kg ASu; B, PET MIP image at 45-60 min post injection, left tumor: HEK::xCT, right tumor: HEK WT; kidneys and bladder are also visible on each image, while pancreas and spleen are visible only in the unblocked condition.

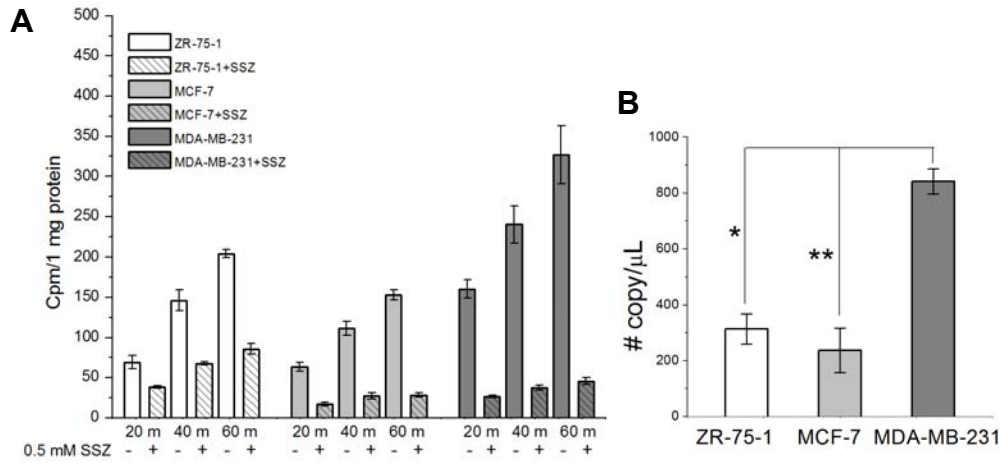


FIGURE 4. A, ^{18}F -FASu uptake in MDA-MB-231, MCF-7 and ZR-75-1 cell lines at 20, 40 and 60 min with and without system x_c^- inhibitor SSZ (0.5 mM); B, xCT mRNA expression levels in ZR-75-1, MCF-7 and MDA-MB-231 cells, * $p < 0.0001$, ** $p < 0.0001$.

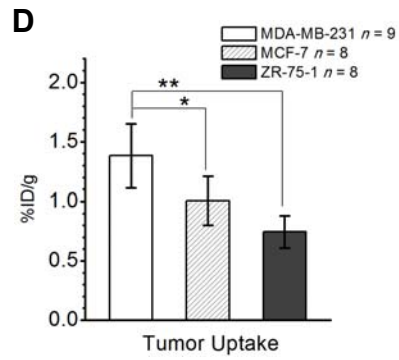
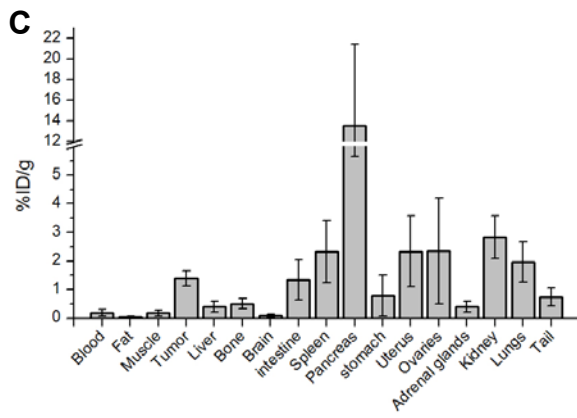
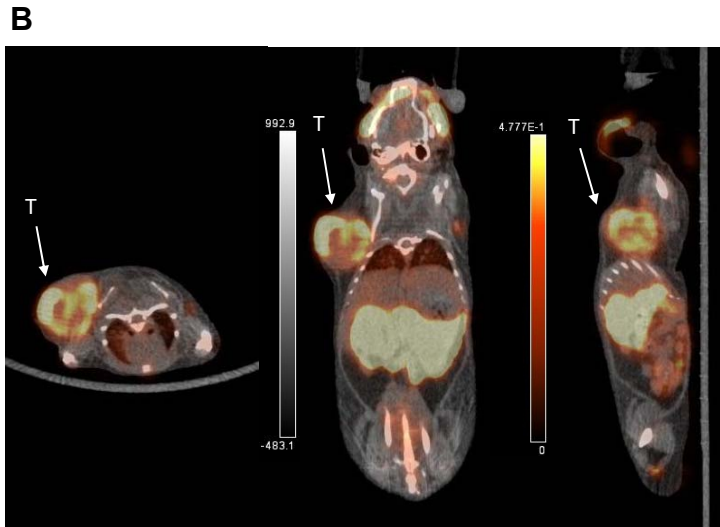
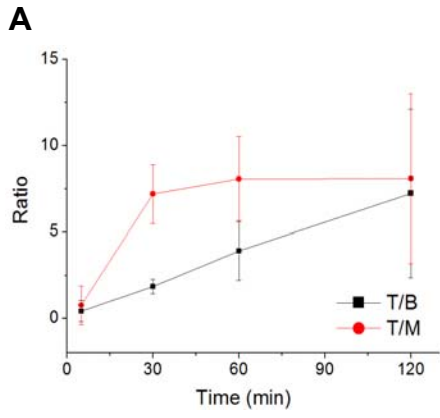


FIGURE 5. ^{18}F -FASu PET image and biodistribution in breast cancer tumor bearing mice. A, Tumor to Blood (T/B) and tumor to muscle (T/M) tracer uptake ratio at various time points in MDA-MB-231 tumor bearing mice; B, PET imaging in a MDA-MB-231 tumor (labeled 'T', left shoulder) bearing mouse at 2 h post injection (fused PET/CT axial, coronal and sagittal slices); C, biodistribution in MDA-MB-231 tumor bearing mice at 2 h post injection; D, comparison of tumor uptake in MDA-MB-231, MCF-7 and ZR-75-1 tumor bearing mice at 2 h post injection, * $p=0.0058$, ** $p<0.0001$.

TABLE 1.

¹⁸F-FASu uptake in MDA-MB-231 in the presence of common amino acid transporters substrates or inhibitors (*n* =4)

	D-Asp	L-Leu	L-Ser	BCH	L-Glu	L-ASu	SSZ	Ctrl
Transporter	EAAT	L, B ⁰ , B ⁰⁺	A, ACS, B ⁰ , B ⁰⁺	L	x _c ⁻ , EAAT, VGLUT	x _c ⁻	x _c ⁻	-
Uptake	119±18%	111±13%	126±14%	115±15%	24±3%	25±3%	14±2%	100%
P value	0.0615	0.1122	0.0043	0.0597	<0.0001	<0.0001	<0.0001	-

¹⁸F-5-fluoro-aminosuberic acid (FASu) as a potential tracer to gauge oxidative stress in breast cancer models

Hua Yang¹, Silvia Jenni², Milena Colovic^{1, 3}, Helen Merkens², Carlee Poleschuk¹, Isabel Rodrigo¹, Qing Miao¹, Bruce F. Johnson⁴, Michael J. Rishel⁴, Vesna Sossi⁵, Jack M. Webster⁴, François Benard^{2, 3}, Paul Schaffer^{1, 3, 6}

Authors' Affiliations: ¹Life Sciences, TRIUMF, Vancouver, Canada; ²The British Columbia Cancer Agency, Vancouver, Canada; ³Department of Radiology, University of British Columbia, Vancouver, Canada; ⁴GE Global Research, Niskayuna, NY, USA; ⁵Department of Physics & Astronomy, University of British Columbia, Vancouver, Canada; and ⁶Department of Chemistry, Simon Fraser University, Vancouver, Canada

For correspondence or reprints contact: Paul Schaffer, Life Sciences, TRIUMF, 4004 Wesbrook Mall, Vancouver, Canada, V6T 2A3. Phone: +1-604-222-7696; Fax: +1-604-222-1074; E-mail: pschaffer@triumf.ca

Supplemental Data

Radiosynthesis of ¹⁸F-FASu

Radiosyntheses were performed on a GE TRACERlab™ FXFN module in a lead-shielded hotcell. Reverse phase high performance liquid (HPLC) chromatography was carried out on an Agilent 1200 series system equipped with a diode array detector and Raytest GABI Star scintillation detector using a Phenomenex Monolithic C₁₈ 4.6 × 100 mm column. Chemicals and reagents were purchased from Sigma Aldrich, Acros Organics and Fisher Scientific. Radiofluorination ¹⁸F⁻ was produced at a TR13 cyclotron from bombardment of H₂¹⁸O at 20 μA. The produced H₂¹⁸O/¹⁸F⁻ was delivered to a GE FXFN automated synthesis module where the ¹⁸F⁻ was trapped on QMA resin. The resin was purged with helium and the fluoride was subsequently released using a mixture of Kryptofix[2.2.2] (K222) (10.1 mg in 200 μL ACN) and K₂CO₃ (2.1 mg in 200 μL water). The solvent was removed by the repeated volatilization of ACN (1.5

mL) under reduced pressure. The precursor (di-tert-butyl 2-((bis-tert-butoxycarbonyl)amino)-5-(tosyloxy)octanedioate, compound **1** Fig. 1B) 1.4 mg was previously dried *in vacuo* and dissolved in 500 μ L anhydrous DMSO in preparation for labeling. The precursor was added to K222/¹⁸F⁻ and reaction was heated at 95°C for 20 min. After which the reaction mixture was cooled to 35°C, diluted by 7 mL H₂O and then loaded onto a Waters tC18 plus Sep-Pak. The Sep-Pak was washed with 17 mL distilled, deionized H₂O and di-tert-butyl 2-((bis-tert-butoxycarbonyl)amino)-5-fluorooctanedioate (compound **2**, Manuscript Fig. 1B) eluted using 1.5 mL ACN. In a separate apparatus, the solvent was removed under the flow of N₂ at 95°C. Trifluoroacetic acid (TFA, 500 μ L) and anisole (8 μ L) were added and the mixture heated at 95°C for 7 min. After TFA was removed *in vacuo*, the residue was dissolved in 0.6 mL PBS and passed through a Waters tC18 light Sep-Pak. The Sep-Pak was washed with an additional 0.6 mL PBS. The combined PBS solution which contained ¹⁸F-FASu was filtered through a 0.22 μ m membrane to generate the final product. Decay corrected radiochemical yield (d.c. RCY) 18 \pm 6% (n=6), radiochemical purity (RCP) >98%, specific activity 17.5 \pm 7 GBq/mmol (n=6). The identities of compound **2** and ¹⁸F-FASu were confirmed by HPLC comparison with the standards.

Quality control of the radiosynthesis was performed by UV and radio-HPLC. The chromatograms are shown below. The retention time difference between the ¹⁸FASu and FASu was 0.27 min, in line with the delay between the UV detector and gamma detector.

HPLC method: Phenomenex Monolithic C18 column, 100 mm \times 4.6 mm, 1 mL/min. A: 0.1% TFA in H₂O, B: 0.1% TFA in ACN. Gradient flow from 100% A at 0 min to 20% A and 80% B in 15 min.

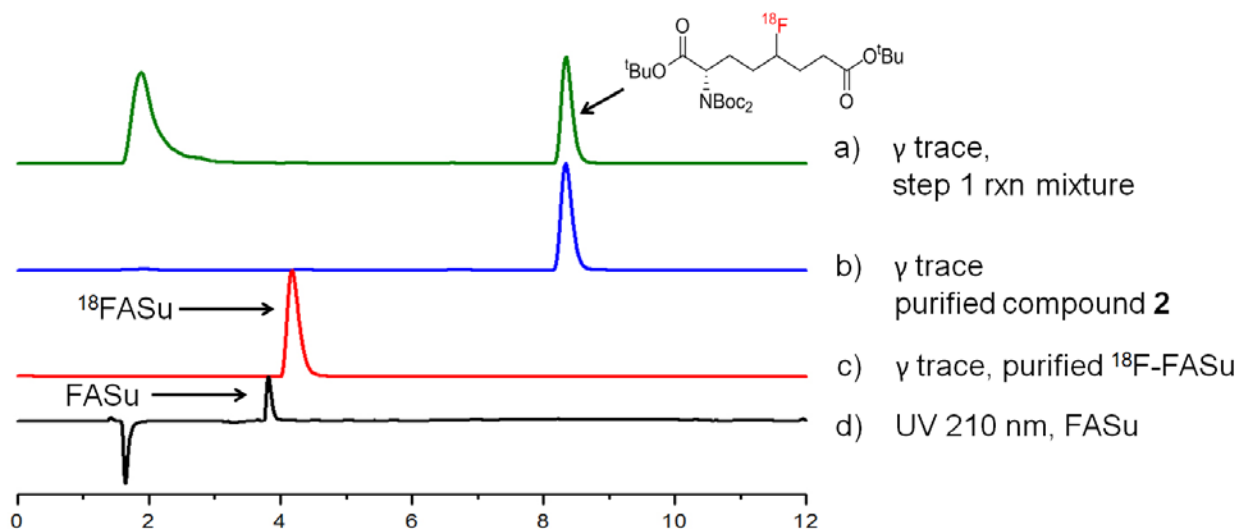


FIGURE 1. HPLC traces of radiosynthesis of ^{18}F -FASu

***In vivo* and *in vitro* stability studies**

For the serum stability study, 0.74 MBq of ^{18}F -FASu in 10 μL PBS was incubated with 100 μL Rag2M plasma for 5, 15, 30, 45, 60, 90 and 120 min. After each incubation, the sample was centrifuged through a 10 kDa molecular weight cut off membrane (Microcon, 14.5k rpm) and analyzed by HPLC. No degradation was observed until 60 min. At 90 min, a small shoulder peak (20%) appeared. At 120 min, the same shoulder peak was observed at 27% compound to primary product peak.

For *in vivo* stability studies, urine and blood samples were collected from two Rag2M mice at 10 and 60 min post injection. The blood samples were centrifuged to collect the serum. Both serum and urine were passed through a 10kDa molecular weight cut off membrane to remove protein followed by HPLC analysis. No metabolites were observed for urine samples at 10 min or 60 min. For the blood samples, no degradation was present at 10 min, and $15.5 \pm 0.5\%$ degradation was observed at 60 min.

Green Fluorescent Protein (GFP) tag of the HEK::xCT

The GFP tag of the HEK::xCT allows the confirmation of the expression of xCT using confocal microscopy.

The GFP and normal image overlay is shown in Supplemental Fig. 2.

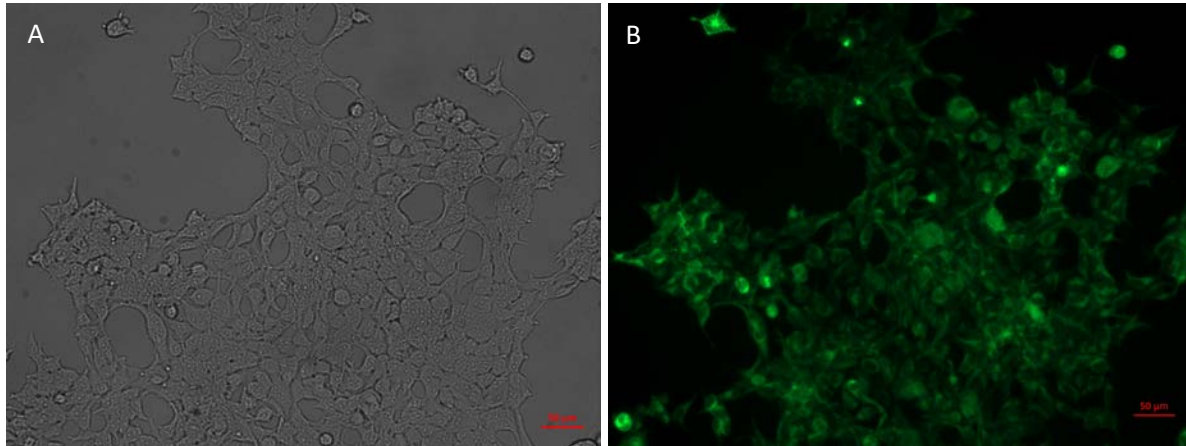


FIGURE 2. Brightfield image (A) and green fluorescent image (B) for HEK::xCT cells. 20x magnification.

Quantitative PCR

IDT PrimeTime® qPCR Primers: *SLC7A11*: Hs.PT.58.38930943; *HPRT1*: Hs.PT.58v.45621572

To construct the *SLC7A11* and *HPRT1* standard curves, total RNA from MDA-MB-231 cells was purified, reverse-transcribed, and *SLC7A11* and *HPRT1* genes were amplified using the same primers as for the qPCR reaction and Q5® High-Fidelity DNA polymerase (New England BioLabs) as per manufacturer's instructions. PCR products were separated on a 2% agarose gel, and target bands were extracted. The DNA was purified using the Monarch® DNA Gel Extraction Kit (New England BioLabs) and quantified using Qubit® dsDNA HS assay kit (Thermo Fisher). Standard curves were constructed using 10-fold serial dilutions and assayed by qPCR in triplicates (Supplemental Fig. 4).

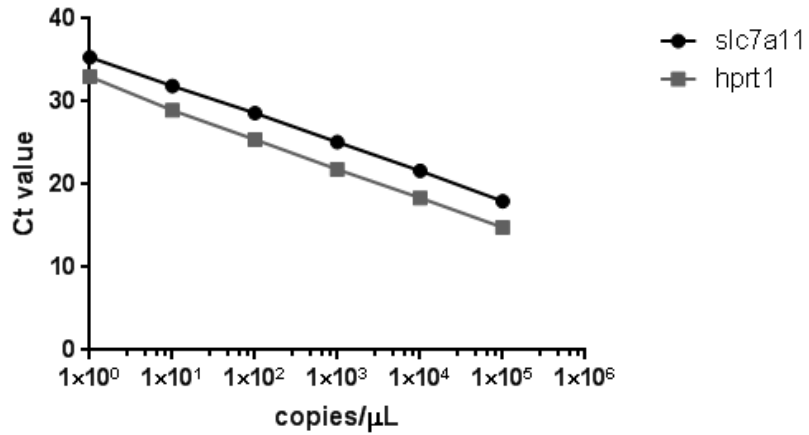


FIGURE 4. Standard curve for absolute qPCR experiments.

TABLE 1: Standard curve parameters

Target	Efficiency (%) (n=3)	R ² (n=3)
SLC7A11	94.720	0.998
HPRT1	89.144	0.998

TABLE 2. PCR cycling conditions

Denaturation	98 °C	30 sec
40 cycles	98 °C	10 sec
	SLC7A11: 60 °C HPRT1: 58 °C	10 sec
	72 °C	20 sec
Final Extension	72 °C	2 min
Hold	4 °C	

TABLE 3: qPCR cycling conditions

Hot Start	95 °C	15 sec
40 cycles	95 °C	10 sec
	SLC7A11: 60 °C HPRT1: 58 °C	60 sec

Biodistribution in MDA-MB-231, MCF-7 and ZR-75-1 tumor bearing mice

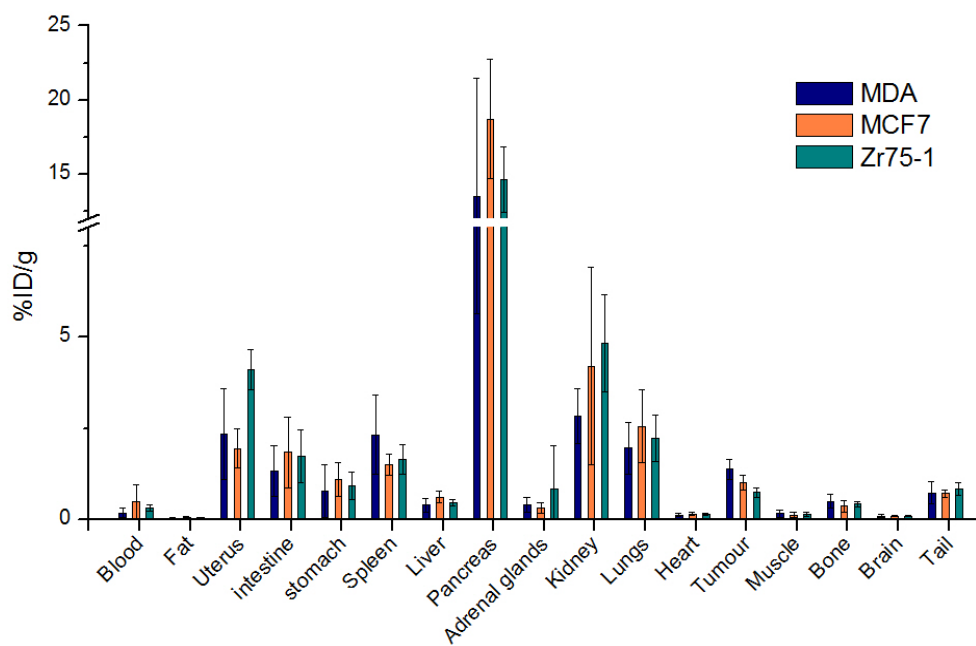


FIGURE 5. Biodistribution of in MDA-MB-231, MCF-7 and ZR-75-1 tumor bearing mice at 2 h post injection. N=9 for MDA-MB-231, n=8 for MCF-7 and ZR-75-1.